Journal of Dental Sciences 20 (2025) 189–200

Available online at www.sciencedirect.com

ScienceDirect

journal homepage: www.e-jds.com

Original Article

Phosphotungstic acid-enhanced micro-computed tomography and RNA sequencing provide a new perspective on temporomandibular joint arthritis induced by complete Freund's adjuvant and collagen-induced arthritis in rat models

Ding-Han Wang [a,b], Kim-Xuyen Nguyen [a], Trang Thi-Ngoc Tran [c], Po-Han Wu [a], Guang Hong [d], Yu-Min Lin [a], Yi-Chen Hsu [a], Cheng-Chieh Yang [a], Yu-Cheng Lin [a], Wun-Eng Hsu [a,e], Ming-Lun Hsu [a*], Mu-Chen Yang [a,f**]

[a] *Department of Dentistry, College of Dentistry, National Yang Ming Chiao Tung University, Taipei, Taiwan*
[b] *Oral Medicine Innovation Center, National Yang Ming Chiao Tung University, Taipei, Taiwan*
[c] *Faculty of Odonto-Stomatology, University of Medicine and Pharmacy, Ho Chi Minh City, Viet Nam*
[d] *Liaison Center for Innovative Dentistry, Graduate School of Dentistry, Tohoku University, Sendai, Japan*
[e] *Department of Dentistry, Far Eastern Memorial Hospital, New Taipei City, Taiwan*
[f] *Division of Craniofacial Development and Tissue Biology, Graduate School of Dentistry, Tohoku University, Sendai, Japan*

Received 18 July 2024; Final revision received 19 August 2024
Available online 28 August 2024

KEYWORDS
Complete Freund's adjuvant-induced arthritis;

Abstract *Background/Purpose:* Temporomandibular joint (TMJ) arthritis causes inflammation and degradation of the mandibular condylar cartilage and subchondral bone. Complete Freund's adjuvant (CFA) and collagen-induced arthritis (CIA) are models for studying TMJ arthritis. While micro-computed tomography (micro-CT) is crucial for three-dimensional (3D)

* Corresponding author. Department of Dentistry, College of Dentistry, National Yang Ming Chiao Tung University, No. 155, Sec. 2, Linong St., Beitou Dist., Taipei 112304, Taiwan.
** Corresponding author. Division of Craniofacial Development and Tissue Biology, Graduate School of Dentistry, Tohoku University, 4-1 Seiryo-machi, Aoba-ku, Sendai 980-8575, Japan.
E-mail addresses: mlhsu@nycu.edu.tw (M.-L. Hsu), yang.mu.chen.c4@tohoku.ac.jp (M.-C. Yang).

https://doi.org/10.1016/j.jds.2024.08.014

Collagen-induced arthritis;
PTA-Enhanced micro-CT;
RNA sequencing;
Temporomandibular joint

bone analysis, it has limitations in imaging nonmineralized tissues. Phosphotungstic acid (PTA) enhances soft tissue contrast. However, research on the 3D imaging of mandibular condylar cartilage and the molecular mechanisms of CFA- and CIA-induced arthritis remains unclear. This study aimed to investigate the bone and PTA-stained cartilage in the mandibular condyle using 3D reconstruction and explore the characteristics of enriched gene ontology terms underlying CFA- and CIA-induced TMJ arthritis in rat models.

Materials and methods: Rat mandibular condyles were collected from control, CFA, and CIA groups. Live micro-CT created 3D bone structures, and PTA-enhanced micro-CT constructed 3D mandibular condylar cartilage. Gene ontology enrichment analysis identified enriched gene ontology terms from differentially expressed genes through RNA sequencing.

Results: Major deformities in cartilage volume and bone morphology were observed in the arthritis-induced groups. The CIA group exhibited significant correlations between cartilage volume and bone parameters changes. Gene ontology enrichment analysis indicated fewer terms with upregulated differentially expressed genes related to inflammation and immune response in the CIA group than in the CFA group.

Conclusion: This study reveals distinct responses between CFA- and CIA-induced TMJ arthritis models. The CIA group exhibited strong correlations between cartilage volume and bone parameter changes and had less pronounced inflammation and immune response than the CFA group.

Introduction

Temporomandibular disorder (TMD) is a multifactorial musculoskeletal disorder that affects the temporomandibular joint (TMJ), masticatory muscles, and adjacent regions.[1] TMD can be categorized into intra-articular and extra-articular types, with the former involving articular disorders such as disc derangement, trauma, and degenerative joint disorders, including arthritis.[2,3] In patients with TMJ arthritis, various proinflammatory cytokines and proteinases are detected in the synovial fluid, resulting in the degradation of the extracellular matrix within the mandibular condylar cartilage.[4] This process also affects the differentiation and activation of osteoclasts, leading to bone erosion.[5]

Micro-computed tomography (micro-CT) is widely used to analyze bone structure with high spatial resolution, allowing precise three-dimensional (3D) analysis. Compared with mineralized tissues, nonmineralized soft tissues exhibit considerably lower X-ray attenuation, which limits their characterization with micro-CT.[6] To address this, many studies have used different contrast agents to identify soft tissue, particularly articular cartilage.[7,8] For instance, phosphotungstic acid (PTA) has been used not only to enhance soft tissue contrast but also to detect collagen distribution in articular cartilage.[9] Although the potential of PTA-enhanced micro-CT as a minimally invasive method for 3D reconstruction of soft tissues,[8] few studies have yet examined the effectiveness of contrast agents in mandibular condylar cartilage.

To understand the mechanisms underlying TMJ arthritis and explore therapeutic strategies, various animal models of TMJ arthritis have been developed. Intra-articular injection of chemical agents, like complete Freund's adjuvant (CFA), is commonly used for its straightforwardness and reproducibility.[10,11] CFA-induced arthritis results in reduced mandibular condylar cartilage thickness, subchondral bone destruction, and inflammatory cell infiltration.[12,13] Collagen-induced arthritis (CIA), using CFA with collagen, also results in degenerative changes in mandibular condylar cartilage.[14,15] Based on previous study, collagen I alone showed no difference in histology or inflammatory mediators compared to the control group.[15] Therefore, CFA is required for CIA-induced arthritis. Although both animal models have been used for a long time, comprehensive studies on the 3D imaging of mandibular condylar cartilage and molecular mechanisms of CFA- and CIA-induced arthritis remains unclear.

RNA sequencing (RNA-Seq) is a powerful genetic analysis technique used to examine the biological characteristics of arthritis-induced models. This technique can be used to identify differentially expressed genes and is often followed by a bioinformatic analysis, such as gene ontology enrichment analysis.[16] This approach can be used to process high-throughput molecular data and generate hypotheses on biological phenomena.[17] In this study, the aim is to investigate the bone and PTA-stained cartilage in the mandibular condyle in 3D reconstruction, and explore the characteristics of enriched gene ontology terms underlying CFA- and CIA-induced TMJ arthritis in rat models. These findings will provide researchers with complete insights into the arthritis-induced models that they use as references.

Materials and methods

Animals

A total of 18 Sprague Dawley rats (female, 250—320 g, 8 weeks old) were randomly divided into three groups, each

comprising six rats following previous study[12] (1) a control group, (2) a CFA group, and (3) a CIA group. On days 0 and 7, bilateral injections of 50 μL of CFA (Sigma–Aldrich, St. Louis, MO, USA) and a 1:1 mixture of 50 μL of CFA with type I collagen (Santa Cruz Biotechnology, Dallas, TX, USA) were administered into the superior space of the TMJ through an anterosuperior puncture technique.[15] The experimental protocols were reviewed and approved by the Institutional Animal Care and Use Committee of National Yang Ming Chiao Tung University, Taipei, Taiwan (IACUC: 1070505r). Fig. 1 shows the conceptual framework of the experiment.

Micro-computed tomography scanning

Live micro-CT scanning was performed on days 0 and 21 to evaluate bone structure, with a total of three rats (six joints) in each group. The rats were intraperitoneally anesthetized using isoflurane and aligned along the vertical axis of the scanner. After scanning on day 21, the rats were euthanized for cartilage evaluation. Bone and cartilage evaluations were conducted using a SkyScan 1276 micro-CT system (Bruker Belgium, Kontich, Belgium), operating at 85 kV with a source current of 200 μA (1-mm Al filter) to capture images with a pixel size of 20 μm.

Phosphotungstic acid -enhanced micro-computed tomography scanning

Rat mandibular condyles were isolated and immersed in 4% formaldehyde and phosphate-buffered saline at room temperature for 24 h. Subsequently, condyles were incubated in a 1% PTA (Sigma–Aldrich) solution at room temperature for another 24 h. PTA-stained cartilage was placed in 70% ethanol and scanned under the same micro-CT scanning conditions.

Micro-computed tomography analysis

Bone

In accordance with the method of a previous study,[13] 3D bone images were first subject to volume of interest segmentation, followed by image processing and then data analysis. Specifically, after segmentation, further analyses were conducted to gather data on various parameters, including bone mineral density, bone volume to tissue volume ratio, trabecular bone thickness, trabecular bone separation, and trabecular bone number.

Cartilage

3D cartilage images underwent preprocessing, image registration, volume of interest segmentation, and data analysis. Custom software efficiently isolated the mandible and reduced 3D points for reconstruction, minimizing computational power and time. Mimics software (21.0) was used for 3D image reconstruction, spatial alignment, and volume of interest segmentation to calculate cartilage volume.

RNA and library preparation

Mandibular condyles from another three rats (six joints) were collected on day 21 and immediately preserved in RNAlater (Thermo Fisher Scientific, Waltham, MA, USA). Sequencing libraries were generated using a KAPA mRNA HyperPrep Kit (Roche, Basel, Switzerland). All procedures were conducted in accordance with the manufacturer's protocol.

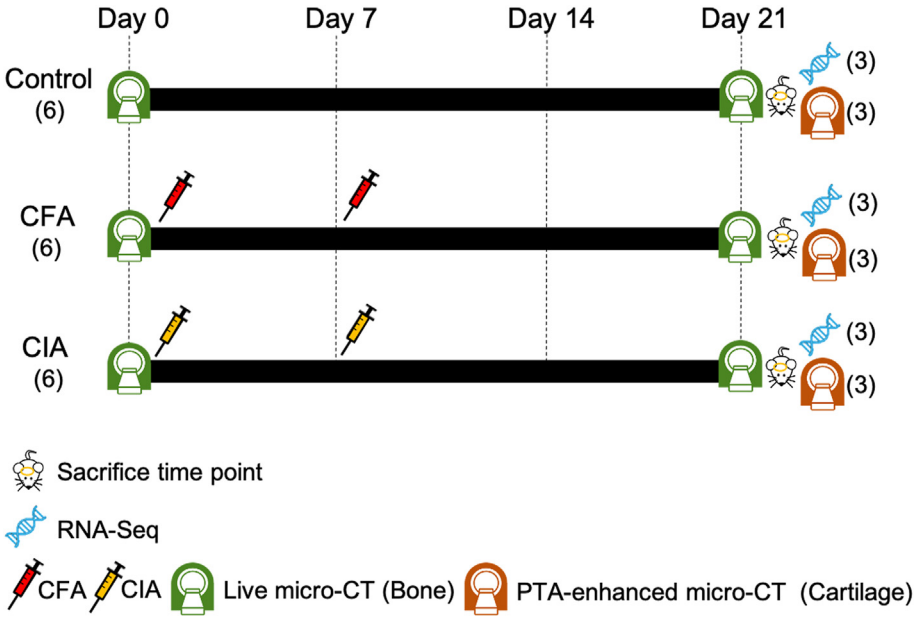

Figure 1 Conceptual framework of the experiment. The rats were divided into three groups: a control group, a CFA group, and a CIA group. Intra-articular injections were administered on days 0 and 7. Live micro-CT was performed on days 0 and 21 for bone evaluation. After the rats were euthanized on day 21, three rats were examined using RNA-Seq, and the remaining rats were evaluated using PTA-enhanced micro-CT for cartilage volume. CFA, complete Freund's adjuvant; CIA, collagen-induced arthritis; Micro-CT, micro-computed tomography; RNA-Seq, RNA sequencing; PTA, phosphotungstic acid.

RNA sequencing analysis

RNA-Seq libraries were sequenced using an Illumina NovaSeq 6000 platform, generating 150-bp paired-end reads. Trimmomatic was used to process raw reads and remove adapter sequences and low-quality bases and reads.[18] After the cleaned reads were aligned to the reference genome by using HISAT2,[19] the aligned reads were processed using featureCounts to obtain raw read counts.[20] Differentially expressed genes were identified using DESeq2 (v.1.26.0).[21] All differentially expressed genes included both upregulated and downregulated genes with a cutoff of |fold change| $>$ 2 and a corrected P value of $<$ 0.01.

Gene ontology enrichment analysis

Gene ontology enrichment analysis was conducted to identify enriched terms associated with both upregulated and downregulated differentially expressed genes. Metascape (http://metascape.org) was used to conduct this analysis, with statistical significance set at P $<$ 0.01.

Statistical analysis

Cartilage volume and bone parameters were shown as mean $\pm$ standard deviation for at least six joints.

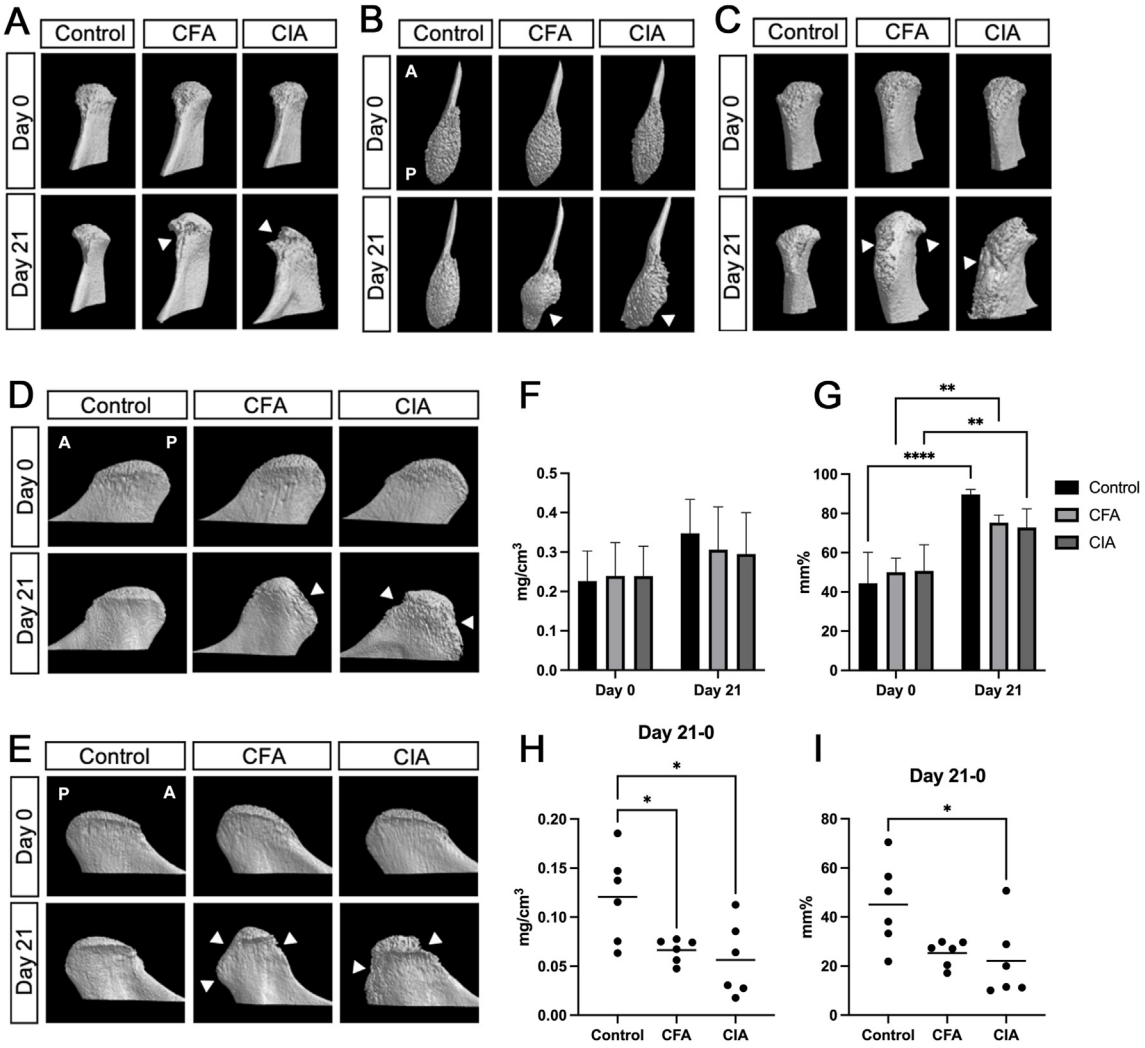

Figure 2 Comparison of mandibular condyle morphology and bone parameters in the CFA, CIA, and control groups. Bone morphology of the three groups was depicted on days 0 and 21 in (A) anterior, (B) superior, (C) posterior, (D) medial, and (E) lateral views. After arthritis induction, significant bone deformation was observed in the arthritis-induced groups in all views. (F) Bone mineral density exhibited an increasing trend over time in all groups. (G) Bone volume to tissue volume ratio significantly increased over time in the three groups. Between days 0 and 21, (H) bone mineral density change significantly decreased in the arthritis-induced groups compared with the control group. (I) Bone volume to tissue volume ratio change significantly decreased in the CIA group compared with the control group. White arrows indicate bone deformation. CFA, complete Freund's adjuvant; CIA, collagen-induced arthritis. A, anterior; P, posterior. *P $<$ 0.05, **P $<$ 0.01, ****P $<$ 0.0001.

Correlations compared cartilage volume on day 21 with percentage changes in bone parameters between day 21 and day 0. All statistical analyses were performed with GraphPad Prism 9 using one-way analysis of variance (ANOVA) with Tukey's post hoc test for cartilage volume and bone parameter changes, and two-way ANOVA with Tukey's post hoc test for bone parameters. Pearson's correlation was used for cartilage and bone parameter change

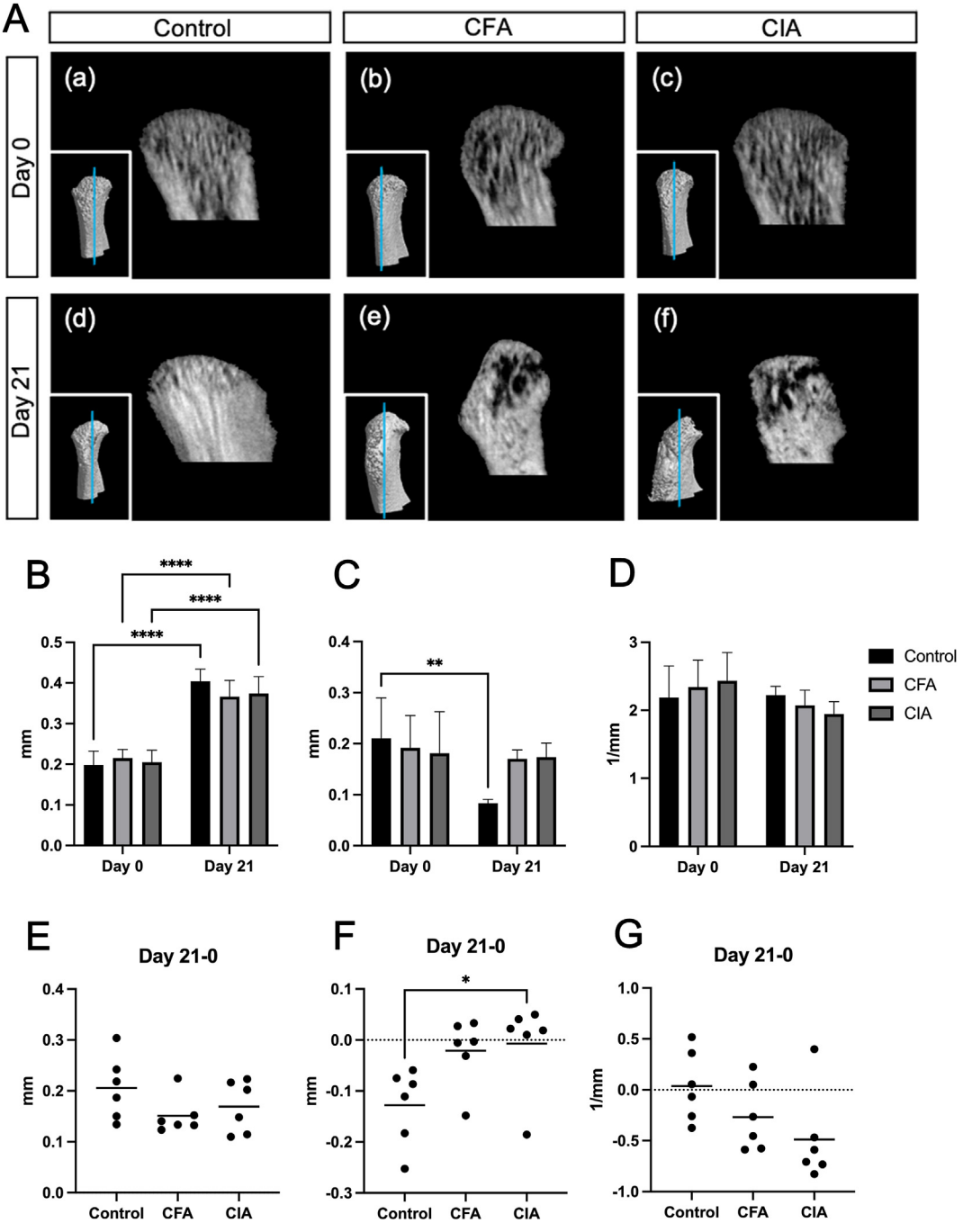

Figure 3 Comparison of subchondral trabecular bone morphology and bone parameters in the CFA, CIA, and control groups. On day 0, no obvious differences were observed in subchondral trabecular bone in the (Aa) control, (Ab) CFA, or (Ac) CIA group. However, on day 21, the density of subchondral trabecular bone in the (Ad) control group substantially increased, whereas the subchondral trabecular bone of the (Ae) CFA and (Af) CIA groups appeared sparser with visible spaces. (B) Trabecular bone thickness significantly increased over time in all groups. (C) Trabecular bone separation significantly decreased in the control group over time. (D) No significant change was observed in trabecular bone number between the three groups. Comparing the parameter changes between day 21 and day 0, no differences were observed in (E) trabecular bone thickness or (G) trabecular bone number among the three groups. However, a significant difference in (F) trabecular bone separation was observed in the CIA group compared to the control group. CFA, complete Freund's adjuvant; CIA, collagen-induced arthritis. *$P < 0.05$, ****$P < 0.0001$.

relationships. Statistical significance levels were $^{*}P < 0.05$, $^{**}P < 0.01$, $^{***}P < 0.001$, and $^{****}P < 0.0001$.

Results

According to the 3D bone image, there were no significant differences in bone morphology among the three groups in the anterior (Fig. 2A), superior (Fig. 2B), posterior (Fig. 2C), medial (Fig. 2D), and lateral (Fig. 2E) views on day 0. After arthritis induction, significant bone deformation was noted in arthritis-induced groups on day 21, particularly in the posterior region, with more distinct changes in the CIA group compared to the CFA group. However, no significant differences were observed in the bone morphology of the control group on day 21 and day 0.

The bone parameters observed on day 0 and day 21 showed no difference in bone mineral density among the three groups (Fig. 2F), while bone volume to tissue volume ratio significantly increased over time in the CFA ($P = 0.0015$), CIA ($P = 0.0068$), and control ($P < 0.0001$) groups (Fig. 2G). Comparing the bone parameter changes between day 21 and day 0, the control group exhibited a significant decrease in bone mineral density compared to both the CFA ($P = 0.0418$) and CIA ($P = 0.0158$) groups (Fig. 2H). In terms of bone volume to tissue volume ratio, a significant decrease was noted between the control and CIA groups ($P = 0.03$, Fig. 2I).

Variations in subchondral trabecular bone within the mandibular condyle were performed on a sagittal central section. No obvious differences were observed in the subchondral trabecular bone among the three group on day 0 (Fig. 3Aa–c). However, on day 21, subchondral trabecular bone density substantially increased in the control group (Fig. 3Ad), while arthritis-induced groups showed sparse and visible spaces (Fig. 3Ae,f). Despite these findings, the differences between the arthritis-induced groups were not significant on day 21.

For bone parameters of subchondral trabecular bone observed on day 0 and day 21, trabecular bone thickness increased over time in all groups ($P < 0.0001$, Fig. 3B), with a significant decrease in trabecular bone separation in the control group ($P = 0.0043$, Fig. 3C). No significant differences were found in trabecular bone number across groups (Fig. 3D). Comparison of bone parameter changes in subchondral trabecular bone on day 21 and day 0 revealed no differences in trabecular bone thickness among the three groups (Fig. 3E). Within these three groups, a progressively increasing trend in trabecular bone separation change was observed. The control group exhibited a significantly lower trabecular bone separation compared to the CIA group ($P < 0.0411$, Fig. 3F). In contrast, a progressively

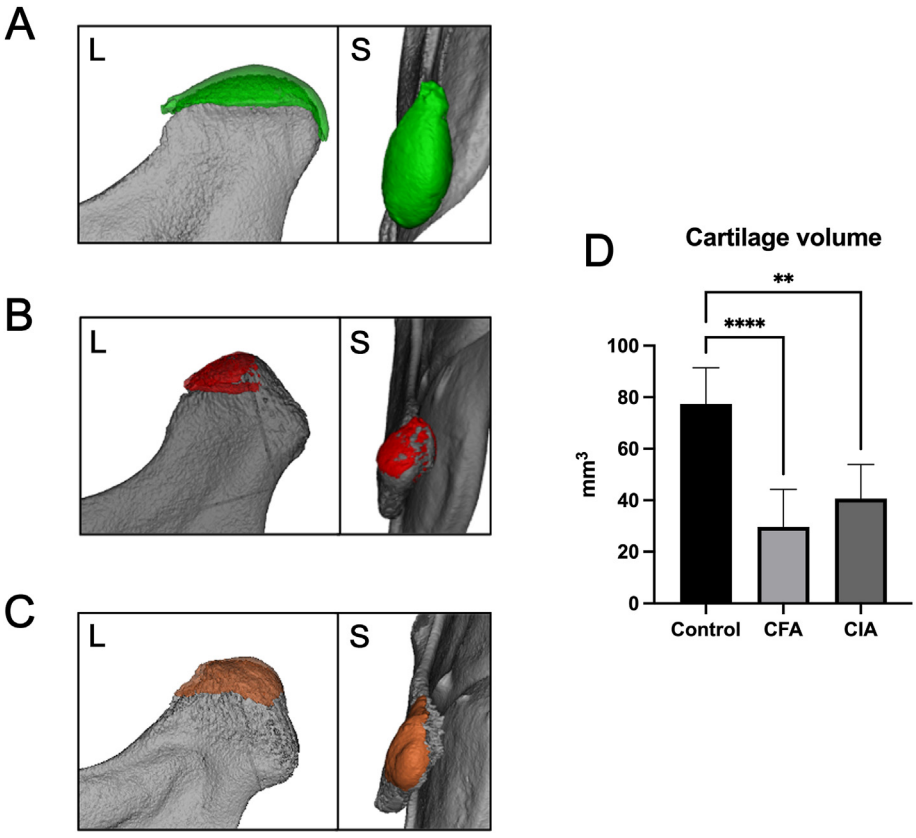

Figure 4 Comparison of cartilage volume at day 21 in the CFA, CIA, and control groups. Lateral and superior views of the 3D reconstruction of cartilage volume in the (A) control, (B) CFA, and (C) CIA groups. (D) A significant decrease was observed in cartilage volume in the CFA and CIA groups. CFA, complete Freund's adjuvant; CIA, collagen-induced arthritis; L, lateral; S, superior. $^{**}P < 0.01$, $^{****}P < 0.0001$.

decreasing trend in trabecular bone number change was found within these three groups (Fig. 3G).

After staining with PTA, the difference between the mandibular condylar cartilage and subchondral bone positions was clearly observed in both the lateral and superior views. In the control group, the mandibular condyle was evenly covered by cartilage (Fig. 4A). Nevertheless, a significant decrease in cartilage volume was observed in both the CFA ($P < 0.0001$) and CIA ($P = 0.0011$) groups (Fig. 4B–D), with the remaining cartilage predominantly located in the anterior mandibular condyle.

Among the control and CFA groups, moderate positive correlations ($0.5 \leq r \leq 0.7$)[22] were noted for bone mineral density ($P = 0.0246$) and bone volume to tissue volume ratio ($P = 0.0176$, Fig. 5A and B), with a moderate negative correlation for trabecular bone separation ($-0.5 \leq r \leq -0.7$, $P = 0.0118$, Fig. 5D). The control and CIA groups showed more significant correlations. Besides to trabecular bone thickness ($P = 0.0343$), which exhibited a moderate positive correlation (Fig. 5H), bone mineral density ($P = 0.0012$), bone volume to tissue volume ratio ($P = 0.0002$), and trabecular bone number ($P = 0.0037$) exhibited high positive correlations ($0.7 \leq r \leq 0.9$, Fig. 5F, G, J). In addition, trabecular bone separation ($-0.9 \leq r \leq -1.0$, $P < 0.0001$) exhibited a very high negative correlation (Fig. 5I).

A comparison of the control and CFA groups, revealed 98 upregulated differentially expressed genes and 88 downregulated differentially expressed genes in the CFA group (Fig. 6A). The upregulated differentially expressed genes were associated with inflammation and immune response more prominently in biological processes than for molecular functions and cellular components (Fig. 6B). Conversely, the downregulated differentially expressed genes associated with muscle fibers across biological processes, molecular functions, and cellular components (Fig. 6C). A comparison of the control and CIA groups revealed 101 upregulated differentially expressed genes and 92 downregulated differentially expressed genes in the CIA group (Fig. 7A). The upregulated differentially expressed genes related to inflammation and immune response, though less distinct than in CFA group (Fig. 7B). The most downregulated differentially expressed genes in CIA were also associated with muscle fibers (Fig. 7C). A comparison of the CFA and CIA groups revealed 44 upregulated differentially expressed genes and 29 downregulated differentially expressed genes in the CIA group (Fig. 8A). The upregulated differentially expressed genes did not show association with inflammation or immune response in biological processes, molecular functions, and cellular components (Fig. 8B), whereas the downregulated differentially expressed genes did (Fig. 8C).

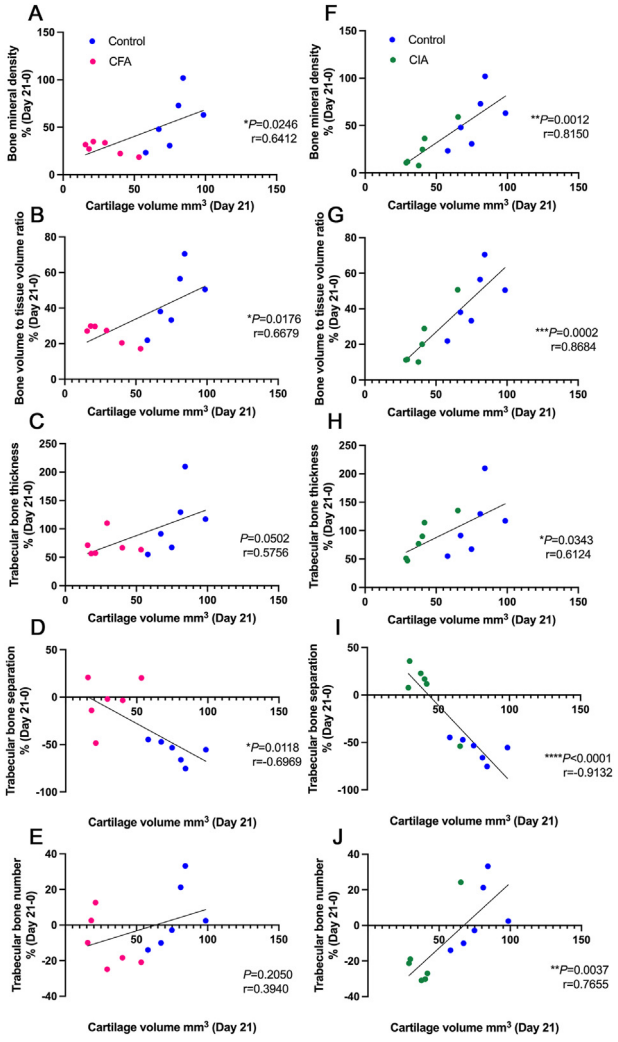

Figure 5 Correlation between cartilage volume and bone parameter changes in the CFA, CIA, and control groups. Among the control and CFA groups, there were moderate positive correlations for (A) bone mineral density and (B) bone volume to tissue volume ratio, and a moderate negative correlation for (D) trabecular bone separation. However, (C) trabecular bone thickness and (E) trabecular bone number did not show significant correlations. In the control and CIA groups, only (H) trabecular bone thickness exhibited a moderate positive correlation, while (F) bone mineral density, (G) bone volume to tissue volume ratio, and (J) trabecular bone number exhibited high positive correlations. Additionally, (I) trabecular bone separation exhibited a very high negative correlation. CFA, complete Freund's adjuvant; CIA, collagen-induced arthritis. *$P < 0.05$, **$P < 0.01$, ***$P < 0.001$, ****$P < 0.0001$.

Discussion

Previous studies have used various contrast agents like ionic contrast agents, uranyl acetate, osmium tetroxide, PTA, and iodine potassium iodide in micro-CT imaging to detect articular cartilage.[7,9,23–25] However, research on contrast enhancement effectiveness in the mandibular condylar cartilage remains limited, focusing mostly on ionic contrast agents and uranyl acetate. Uranyl acetate offers strong cartilage visibility but is toxic, while PTA is less toxic.[7,26,27] PTA, as an anionic contrast agent, selectively binds to positively charged collagen groups and cause minimal tissue shrinkage.[25,28] In 2015, PTA was recognized as a potential marker for visualizing collagen distribution in articular cartilage through 3D reconstruction without compromising tissue integrity.[9] Through PubMed advanced search, we found that most studies on PTA in articular cartilage are related to knee joints, including in mice or humans.[9,29]

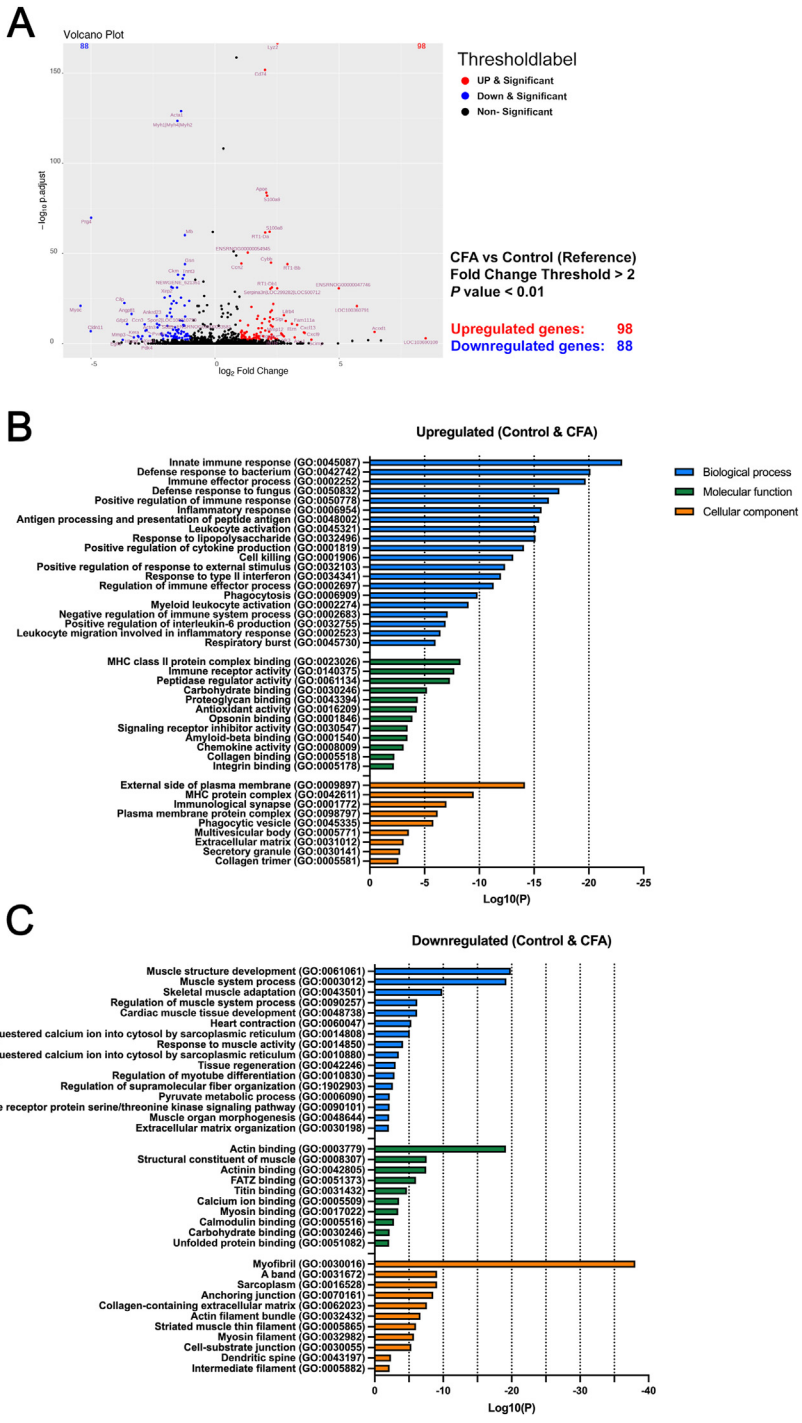

Figure 6 Gene ontology enrichment analysis of differentially expressed genes in the control and CFA groups. (A) The number of upregulated and downregulated differentially expressed genes was compared between the control and CFA groups. (B) The upregulated differentially expressed genes in biological processes, molecular functions, and cellular components were associated with inflammation and immune response. (C) The downregulated differentially expressed genes in biological processes, molecular functions, and cellular components were associated with muscle fibers or other terms. CFA, complete Freund's adjuvant; CIA, collagen-induced arthritis.

Currently, there are no studies on the application of PTA in mandibular condylar cartilage. Therefore, to the best of the authors' knowledge, this study is the first to use PTA as a contrast agent to assess cartilage volume in rat mandibular condyles.

3D imaging revealed significant bone and cartilage damage in the arthritis-induced group. The anterior mandibular condyle, identified as a high-stress region due to unique TMJ movement patterns, undergoes remodeling to balance mechanical load.[30–32] Remodeling modulates

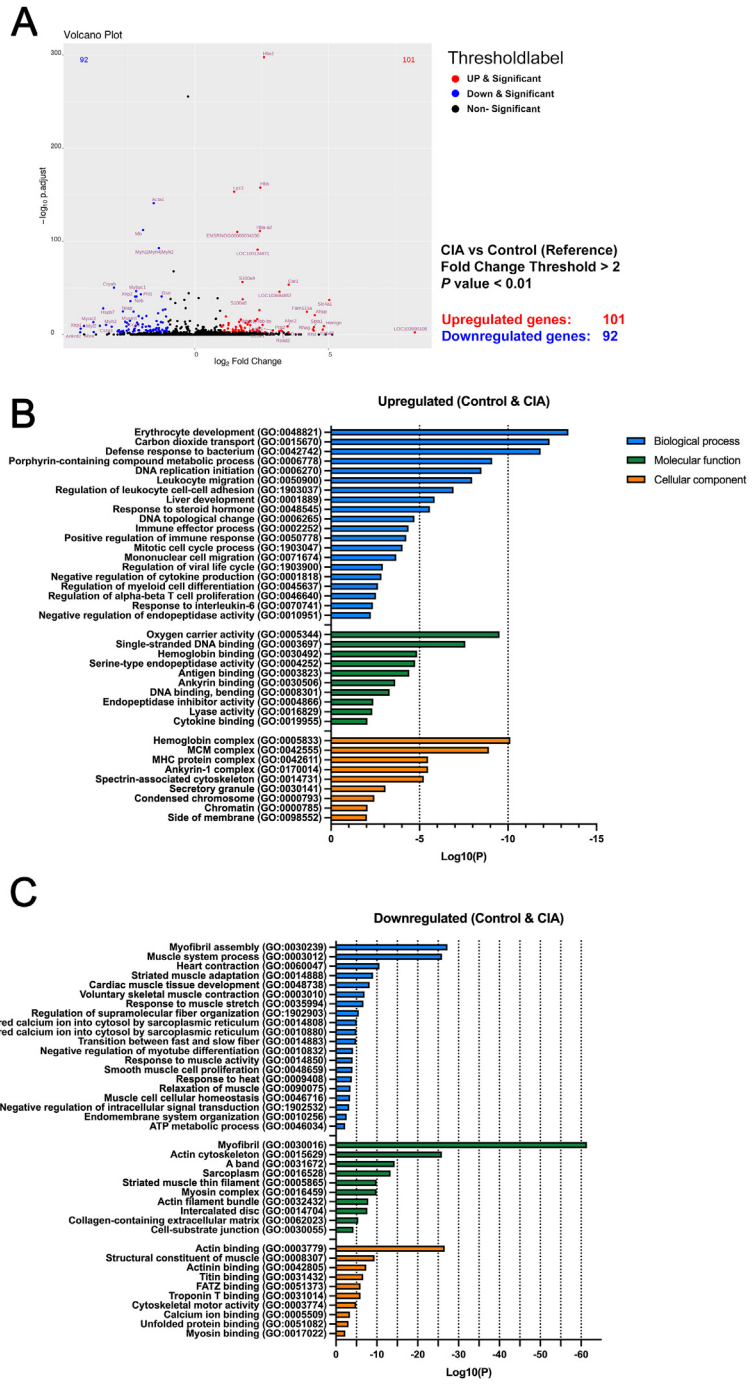

Figure 7 Gene ontology enrichment analysis of differentially expressed genes in the control and CIA groups. (A) The number of upregulated and downregulated differentially expressed genes was compared between the control and CIA groups. (B) The upregulated differentially expressed genes in biological processes and cellular components were associated with inflammation and immune response. However, for molecular functions, no key gene ontology terms associated with inflammation or immune response were observed. (C) The downregulated differentially expressed genes in biological processes, molecular functions, and cellular components were associated with muscle fibers or other terms. CFA, complete Freund's adjuvant; CIA, collagen-induced arthritis.

chondrogenesis or the composition of extracellular matrix to achieve a better balance,[32,33] leading to a concentration of cartilage in this area. Under overloading stress, cartilage degradation and subchondral bone resorption occur in the posterior mandibular condyle.[34] This may explain why, in this study, damage to both bone and cartilage was more pronounced in the posterior region than in the anterior region. Inflammatory factors may affect bone growth, thereby influencing bone remodeling capacity.[35] The correlation between cartilage volume and bone parameter changes indicated that smaller cartilage volume was associated with minimal bone parameter changes in the

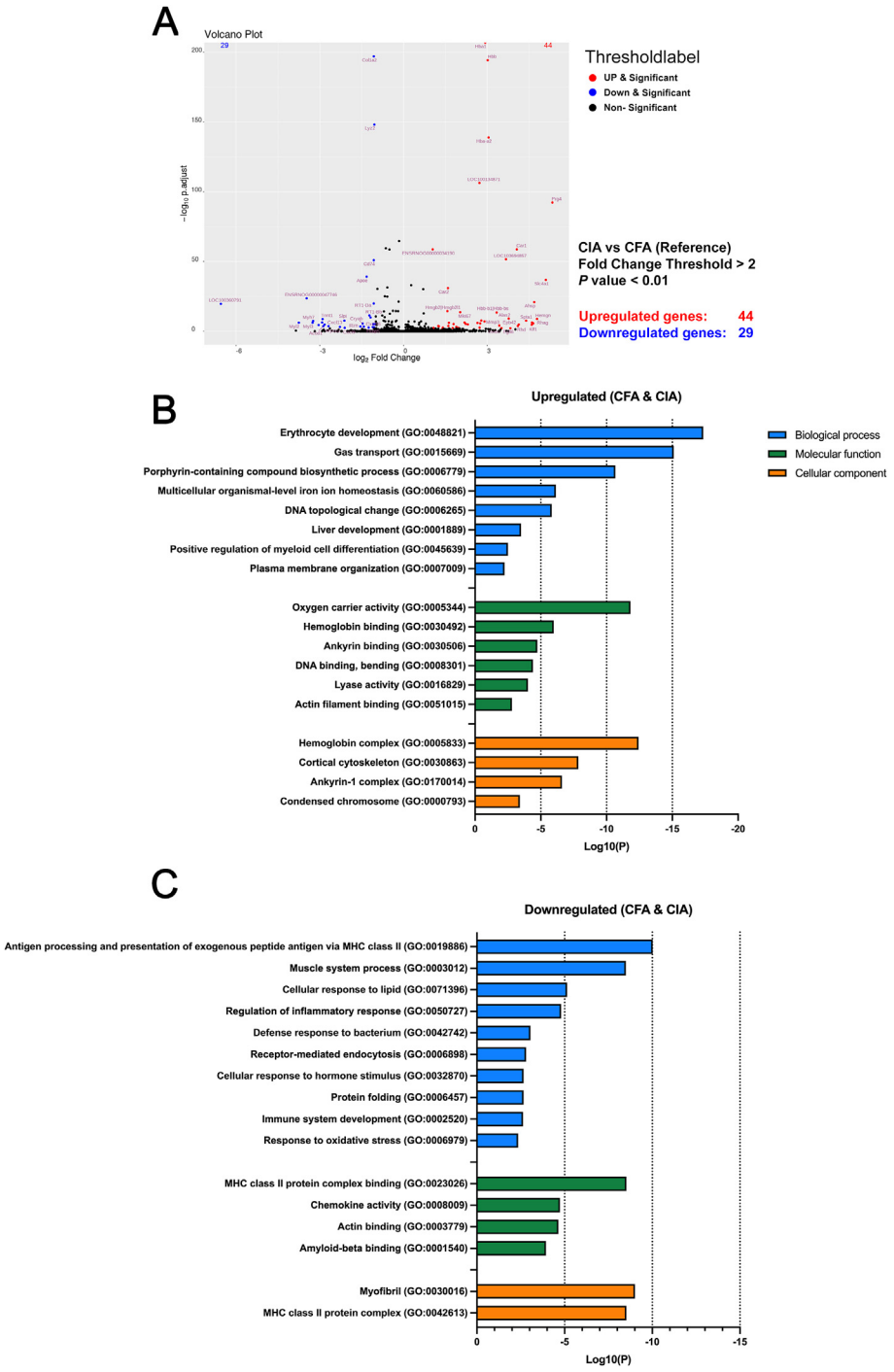

Figure 8 Gene ontology enrichment analysis of differentially expressed genes in the CFA and CIA groups. (A) The number of upregulated and downregulated differentially expressed genes was compared between the CFA and CIA groups. (B) The upregulated differentially expressed genes with enriched gene ontology terms in biological processes, molecular functions, and cellular components were not associated with inflammation or immune response, whereas (C) the downregulated differentially expressed genes were. CFA, complete Freund's adjuvant; CIA, collagen-induced arthritis

arthritis-induced group, suggesting lower remodeling capacity. The CIA group showed a stronger correlation than the CFA group, indicating lower remodeling capacity in the CIA group. However, the limitation of 3D imaging is that it can only show overall changes; therefore, detailed internal tissue changes require histological analysis for further verification.

Previous studies suggest CIA-induced arthritis models exhibit RA-like pathological mechanisms,[36,37] while the type of arthritis induced by CFA is controversial.[11,38] Although the type of CFA-induced arthritis could not be clearly defined in this study, gene enrichment analysis was used to explore the differences in enriched gene ontology terms between the CFA- and CIA-induced models. Gene

ontology categorizes gene functions into molecular function, cellular component, and biological process, reflecting molecular—level activities, locations, and contributions to biological objectives, respectively.[39,40] Based on the study findings, gene ontology terms related to inflammation and immune response were identified among the upregulated differentially expressed genes compared to the control group in the arthritis-induced groups. However, the expression level of these gene ontology terms was lower in the CIA group. Additionally, gene ontology terms associated with inflammation and immune response were found among the downregulated differentially expressed genes in the CIA group compared to the CFA group on day 21. Furthermore, previous histological results indicated more distinct changes in the mandibular condylar cartilage in the CFA group, whereas the CIA group showed less cellularity and thinning of the mandibular condylar cartilage on day 35.[15] These observations suggest that the inflammatory response in CIA was less sustained but resulted in more severe tissue damage.

In conclusion, the arthritis-induced groups showed significant deformities in cartilage volume and bone morphology. The CIA group exhibited strong correlations between cartilage volume and bone parameter changes and had less pronounced inflammation and immune response than the CFA group. These findings provide comprehensive insights for researchers seeking to utilize these arthritis-induced models as reference models.

Declaration of competing interest

The authors have no conflicts of interest relevant to this article.

Acknowledgments

This study was supported by the Ministry of Science and Technology (MOST111-2314-B-A49-033), the National Science and Technology Council of Taiwan (NSTC112-2314-B-A49-058 and NSTC112-2314-B-A49-027), and the Higher Education Sprout Project of the National Yang Ming Chiao Tung University and Ministry of Education (MOE), Taiwan. The authors would like to sincerely thank the Taiwan Mouse Clinic, Academia Sinica, and Taiwan Animal Consortium for their technical support in micro-CT scanning and to thank the BIOTOOLS for their assistance in RNA-Seq analysis. This manuscript was edited by Wallace Academic Editing.

References

1. Chang CL, Wang DH, Yang MC, Hsu WE, Hsu ML. Functional disorders of the temporomandibular joints: internal derangement of the temporomandibular joint. *Kaohsiung J Med Sci* 2018;34:223—30.
2. Gauer RL, Semidey MJ. Diagnosis and treatment of temporomandibular disorders. *Am Fam Physician* 2015;91:378—86.
3. Lomas J, Gurgenci T, Jackson C, Campbell D. Temporomandibular dysfunction. *Aust J Gen Pract* 2018;47:212—5.
4. Zwiri A, Al-Hatamleh MAI, W Ahmad WMA, et al. Biomarkers for temporomandibular disorders: current status and future directions. *Diagnostics* 2020;10:303.
5. Tanaka E, Detamore MS, Mercuri LG. Degenerative disorders of the temporomandibular joint: etiology, diagnosis, and treatment. *J Dent Res* 2008;87:296—307.
6. Heimel P, Swiadek NV, Slezak P, et al. Iodine-enhanced micro-CT imaging of soft tissue on the example of peripheral nerve regeneration. *Contrast Media Mol Imaging* 2019;2019:7483745.
7. Kun-Darbois JD, Manero F, Rony L, Chappard D. Contrast enhancement with uranyl acetate allows quantitative analysis of the articular cartilage by microCT: application to mandibular condyles in the BTX rat model of disuse. *Micron* 2017;97:35—40.
8. O J, Kwon HJ, Cho TH, Woo SH, Rhee YH, Yang HM. Micro-computed tomography with contrast enhancement: an excellent technique for soft tissue examination in humans. *PLoS One* 2021;16:e0254264.
9. Nieminen HJ, Ylitalo T, Karhula S, et al. Determining collagen distribution in articular cartilage using contrast-enhanced micro-computed tomography. *Osteoarthritis Cartilage* 2015;23:1613—21.
10. Wang D, Qi Y, Wang Z, Guo A, Xu Y, Zhang Y. Recent advances in animal models, diagnosis, and treatment of temporomandibular joint osteoarthritis. *Tissue Eng Part B* 2023;29:62—77.
11. Noh ASM, Chuan TD, Khir NAM, et al. Effects of different doses of complete Freund's adjuvant on nociceptive behaviour and inflammatory parameters in polyarthritic rat model mimicking rheumatoid arthritis. *PLoS One* 2021;16:e0260423.
12. Yang MC, Wang DH, Cherng JH, et al. Role of link N in modulating inflammatory conditions. *J Oral Facial Pain Headache* 2019;33:114—22.
13. Thi Ngoc TT, Wang DH, Yang MC, et al. Effects of food hardness on temporomandibular joint osteoarthritis: qualitative and quantitative micro-CT analysis of rats in vivo. *Ann Anat* 2022;246:152029.
14. Crossman J, Lai H, Kulka M, Jomha N, Flood P, El-Bialy T. Collagen-induced temporomandibular joint arthritis juvenile rat animal model. *Tissue Eng C Methods* 2021;27:115—23.
15. Wang DH, Yang MC, Hsu WE, Hsu ML, Yu LM. Response of the temporomandibular joint tissue of rats to rheumatoid arthritis induction methods. *J Dent Sci* 2017;12:83—90.
16. Young MD, Wakefield MJ, Smyth GK, Oshlack A. Gene ontology analysis for RNA-seq: accounting for selection bias. *Genome Biol* 2010;11:R14.
17. Tomczak A, Mortensen JM, Winnenburg R, et al. Interpretation of biological experiments changes with evolution of the gene ontology and its annotations. *Sci Rep* 2018;8:5115.
18. Bolger AM, Lohse M, Usadel B. Trimmomatic: a flexible trimmer for illumina sequence data. *Bioinformatics* 2014;30:2114—20.
19. Kim D, Paggi JM, Park C, Bennett C, Salzberg SL. Graph-based genome alignment and genotyping with HISAT2 and HISAT-genotype. *Nat Biotechnol* 2019;37:907—15.
20. Liao Y, Smyth GK, Shi W. FeatureCounts: an efficient general purpose program for assigning sequence reads to genomic features. *Bioinformatics* 2014;30:923—30.
21. Love MI, Huber W, Anders S. Moderated estimation of fold change and dispersion for RNA-seq data with DESeq2. *Genome Biol* 2014;15:550.
22. Mukaka MM. Statistics corner: a guide to appropriate use of correlation coefficient in medical research. *Malawi Med J* 2012;24:69—71.
23. Ruan MZ, Dawson B, Jiang MM, Gannon F, Heggeness M, Lee BH. Quantitative imaging of murine osteoarthritic cartilage by phase-contrast micro-computed tomography. *Arthritis Rheum* 2013;65:388—96.
24. Renders GA, Mulder L, Lin AS, et al. Contrast-enhanced microCT (EPIC-muCT) ex vivo applied to the mouse and human jaw joint. *Dentomaxillofacial Radiol* 2014;43:20130098.
25. Lesciotto KM, Motch Perrine SM, Kawasaki M, et al. Phosphotungstic acid-enhanced microCT: optimized protocols for

embryonic and early postnatal mice. *Dev Dynam* 2020;249:573—85.
26. Baerlocher MO, Asch M, Myers A. The use of contrast media. *CMAJ (Can Med Assoc J)* 2010;182:697.
27. Kwon KA, Bax DV, Shepherd JH, Cameron RE, Best SM. Avoiding artefacts in microCT imaging of collagen scaffolds: effect of phosphotungstic acid (PTA)-staining and crosslink density. *Bioact Mater* 2022;8:210—9.
28. Quintarelli G, Zito R, Cifonelli JA. On phosphotungstic acid staining. I. *J Histochem Cytochem* 1971;19:641—7.
29. Das Neves Borges P, Forte AE, Vincent TL, Dini D, Marenzana M. Rapid, automated imaging of mouse articular cartilage by microCT for early detection of osteoarthritis and finite element modelling of joint mechanics. *Osteoarthritis Cartilage* 2014;22:1419—28.
30. Helland MM. Anatomy and function of the temporomandibular joint. *J Orthop Sports Phys Ther* 1980;1:145—52.
31. Shao B, Teng H, Dong S, Liu Z. Finite element contact stress analysis of the temporomandibular joints of patients with temporomandibular disorders under mastication. *Comput Methods Progr Biomed* 2022;213:106526.
32. Sobue T, Yeh WC, Chhibber A, et al. Murine TMJ loading causes increased proliferation and chondrocyte maturation. *J Dent Res* 2011;90:512—6.
33. Shen G, Darendeliler MA. The adaptive remodeling of condylar cartilage—a transition from chondrogenesis to osteogenesis. *J Dent Res* 2005;84:691—9.
34. Fang L, Ye Y, Tan X, Huang L, He Y. Overloading stress-induced progressive degeneration and self-repair in condylar cartilage. *Ann N Y Acad Sci* 2021;1503:72—87.
35. Skerry TM. The effects of the inflammatory response on bone growth. *Eur J Clin Nutr* 1994;48(Suppl 1):S190—7. discussion S98.
36. Luan J, Hu Z, Cheng J, et al. Applicability and implementation of the collagen-induced arthritis mouse model, including protocols. *Exp Ther Med* 2021;22:939.
37. Brand DD, Latham KA, Rosloniec EF. Collagen-induced arthritis. *Nat Protoc* 2007;2:1269—75.
38. Ismail CAN, Mohd Noh AS, Tan DC, Mohamed Khir NA, Shafin N. A review on complete Freund's adjuvant-induced arthritic rat model: factors leading to its success. *IIUM Med J Malays* 2022;21:1—12.
39. Gene Ontology C, Aleksander SA, Balhoff J, et al. The gene ontology knowledgebase in 2023. *Genetics* 2023;224:iyad031.
40. Thomas PD. The gene ontology and the meaning of biological function. *Methods Mol Biol* 2017;1446:15—24.